

BRIEF NOTES • OPEN ACCESS

Fabrication of ordered Fe–Ni nitride film with equiatomic Fe/Ni ratio

To cite this article: Fumiya Takata *et al* 2018 *Jpn. J. Appl. Phys.* **57** 058004

View the [article online](#) for updates and enhancements.

Related content

- [L₁₀-ordered FeNi film grown on Cu–Ni binary buffer layer](#)
T Kojima, M Mizuguchi and K Takanashi
- [Magnetic Anisotropy and Chemical Order of Artificially Synthesized L₁₀-Ordered FeNi Films on Au–Cu–Ni Buffer Layers](#)
Takayuki Kojima, Masaki Mizuguchi, Tomoyuki Koganezawa *et al.*
- [Epitaxial growth of ferromagnetic Fe_xN thin films on SrTiO₃\(001\) substrates by molecular beam epitaxy](#)
K Ito, G H Lee and T Suemasu



Fabrication of ordered Fe–Ni nitride film with equiatomic Fe/Ni ratio

Fumiya Takata, Keita Ito, and Takashi Suemasu*

Institute of Applied Physics, Graduate School of Pure and Applied Sciences, University of Tsukuba, Tsukuba, Ibaraki 305-8573, Japan

*E-mail: suemasu@bk.tsukuba.ac.jp

Received January 24, 2018; accepted March 16, 2018; published online April 16, 2018

We successfully grew a single-phase tetragonal FeNiN film with an equiatomic ratio of Fe, Ni, and N on a MgO(001) substrate by molecular beam epitaxy. We then demonstrated the formation of Fe₂Ni₂N films by extracting N atoms from the FeNiN film. These results suggested that Fe and Ni atoms in the Fe₂Ni₂N film were L1₀-ordered along the film plane direction because of the *a*-axis orientation growth of the FeNiN film on the MgO(001) substrate. © 2018 The Japan Society of Applied Physics

Fe–Ni nitrides have attracted much interest owing to the rich variety in their magnetic and transport properties.^{1–10} In particular, anti-perovskite type cubic Fe–Ni nitride Fe_{4–*x*}Ni_{*x*}N, where the metallic atoms form an fcc lattice with a N atom positioned at a body-center position, have been extensively studied not only for magnetic materials but also for spintronic applications. For example, Fe₄N has been theoretically predicted to have a very large negative spin-polarization of electrical conductivity,¹¹ and its high spin-polarization has been experimentally demonstrated by the point-contact Andreev reflection technique and the tunneling magnetoresistance effect.^{12,13} It is reported that substitution of Ni for Fe atoms improves the chemical stability and mechanical ductility of these materials,^{6,7} and modifies their magnetic and electronic structure.⁵ The saturation magnetization (*M_S*) and lattice constant tend to decrease with increasing the Ni content.⁸ According to a Mössbauer study and first-principle calculations, Ni atoms likely occupy corner sites.^{9,10} Recently, our group and another showed that FeNi₃N has a larger negative spin-polarization of its density of states at the Fermi level than that of Fe₄N, and was thus suggested to be a high spin-polarized material.^{14,15} Previously, we succeeded in growing Fe_{4–*x*}Ni_{*x*}N (*x* = 0, 1, 3, and 4) epitaxial films on a SrTiO₃(001) substrate by molecular beam epitaxy (MBE), and investigated their structure, magnetic properties, and magnetotransport properties in detail.^{15–17}

Another Fe–Ni nitride phase with an equiatomic ratio of Fe, Ni, and N, namely FeNiN, was discovered by Arnott and Wold during the nitriding process of Fe₂Ni₂N powders. The crystal structure was determined to be face-centered tetragonal (space group: *P4/mmm*) with lattice parameters of *a* (in-plane) = 4.002 Å, *c* (out-of-plane) = 3.713 Å, and *c/a* = 0.928 as shown in Fig. 1(a).¹⁸ A notable feature of this phase is the atomic ordering of Fe and Ni atoms, namely, Fe and Ni monolayers alternately stack along the *c*-axis direction, which form a so-called L1₀ structure, with N atoms located side by side with Fe atoms. Quite recently, Goto et al. pointed out that FeNiN is an important intermediate phase for obtaining single-phase L1₀-FeNi,¹⁹ which is a promising material from the perspective of both rare-earth free permanent magnets and ferromagnetic films with perpendicular magnetic anisotropy (PMA). These phenomena can be attributed to its large uniaxial magnetic anisotropy appearing in the *c*-axis direction.²⁰ According to Goto et al., N atoms diffuse out without

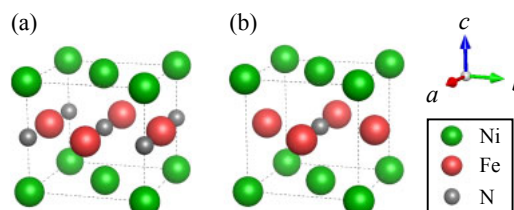


Fig. 1. (Color online) Crystal structure of (a) FeNiN and (b) Fe₂Ni₂N.

disturbing the atomic ordering of the Fe and Ni atoms during the denitriding process, and therefore highly ordered L1₀-FeNi alloy powder can be obtained. These interesting phenomena motivated us to fabricate FeNiN epitaxial films and then extract N atoms from the FeNiN film. There have been no reports thus far on the formation of FeNiN films. In this study, we grew FeNiN films, and demonstrated the fabrication of a Fe₂Ni₂N film, as shown in Fig. 1(b), by extracting N atoms from FeNiN films.

40-nm thick FeNiN films were grown on MgO(001) single-crystal substrates by MBE with the use of solid Fe and Ni sources, and a radio-frequency N₂ plasma. We followed the same growth condition as that for Fe_{4–*x*}Ni_{*x*}N films,¹⁵ and controlled the crucibles temperatures of Fe and Ni, setting their atomic ratio to be 1 : 1. The total deposition rate was set at 0.5 nm/min, which was half that of Fe_{4–*x*}Ni_{*x*}N films. The substrate temperature (*T_S*) was varied from 200 to 450 °C. A 3 nm-thick SiO₂ capping layer was in situ deposited by sputtering. N extraction was performed by annealing under vacuum for 30 min at an annealing temperature in the range of *T_A* of 300–400 °C. The crystalline qualities and structures were characterized by reflection high-energy electron diffraction (RHEED), out-of-plane (*2θ*–*ω*) X-ray diffraction (XRD), and in-plane (*2θ_χ*–*φ*) XRD measurements with Cu-*Kα* radiation. The magnetic properties were measured with a vibrating sample magnetometer at room temperature.

Figure 2 shows the out-of-plane and in-plane XRD profiles and RHEED patterns of the samples grown at *T_S* = 200, 300, and 450 °C. The incident electron beam was set along the MgO[100] azimuth. When the *T_S* were 200 and 300 °C, XRD peaks originating only from FeNiN were observed. The (*h*00)-oriented peaks were confirmed in the out-of-plane XRD, whereas (0*k*0)- and (00*l*)-oriented peaks appeared in the in-plane XRD profiles when the X-ray scattering vector (*Q*) was set to MgO[200]. These results verified the epitaxial



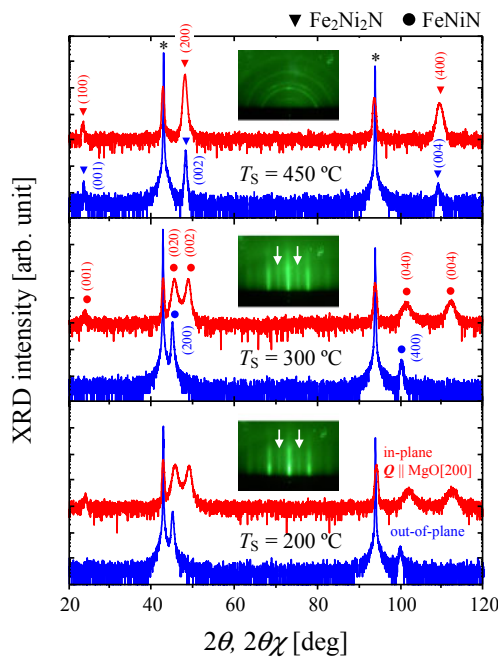


Fig. 2. (Color online) Out-of-plane (blue, lower) and in-plane XRD (red, upper) and RHEED patterns of samples grown at $T_S = 200, 300,$ and 450 °C. Asterisks indicate diffraction peaks from the substrate.

growth of single-phase FeNiN films on MgO(001) with an epitaxial relationship of FeNiN[001](100) \parallel MgO[100](001) and FeNiN[010](100) \parallel MgO[100](001). An FeNiN film consists of two variants, whose c -axis was in-plane and rotated around the film normal by 90° each other. However, this epitaxial relationship is different from our prediction that the favored epitaxial relationship would be FeNiN[100](001) \parallel MgO[100](001), i.e., a cube-on-cube relationship, with the smallest lattice mismatch of approximately -5% . The RHEED results clearly show streaky patterns together with superlattice streaks, as indicated by arrows in Fig. 2, owing to a long-range order of the N atoms. The lattice constants were calculated to be $a = 4.01$ Å, $c = 3.71$ Å, and $c/a = 0.925$, which are close to those reported.¹⁸⁾ For the sample grown at $T_S = 450$ °C, both the out-of-plane and in-plane XRD patterns indicate the c -axis-oriented epitaxial growth of Fe₂Ni₂N; however, the RHEED pattern changed from streaky to a ring shape. These results show the coexistence of epitaxial Fe₂Ni₂N grains and non-epitaxial ones in the grown film. The superlattice diffractions of the Fe₂Ni₂N(001) and (100) indicated a long-range order of N atoms at body-center sites.¹⁵⁾ The order parameter of N body-center site (S_N) was calculated to be 0.77 using the superlattice diffraction of Fe₂Ni₂N(100) and the fundamental diffraction of Fe₂Ni₂N(200).¹⁵⁾ We considered that N atoms diffused from the FeNiN film at elevated T_S to form Fe₂Ni₂N. The obtained Fe₂Ni₂N film had a cubic structure with $a = 3.776$ Å, $c = 3.779$ Å, and $c/a = 1.001$. We note that it was necessary to grow a c -axis oriented FeNiN film to obtain an L1₀-FeNi film with PMA through N extraction. Thus, further studies on the growth of FeNiN films with c -axis orientation are required in future work.

Next, we attempted to extract N atoms from the FeNiN film. We selected FeNiN films grown at $T_S = 200$ °C based on the XRD results shown in Fig. 2. Figure 3 shows the out-

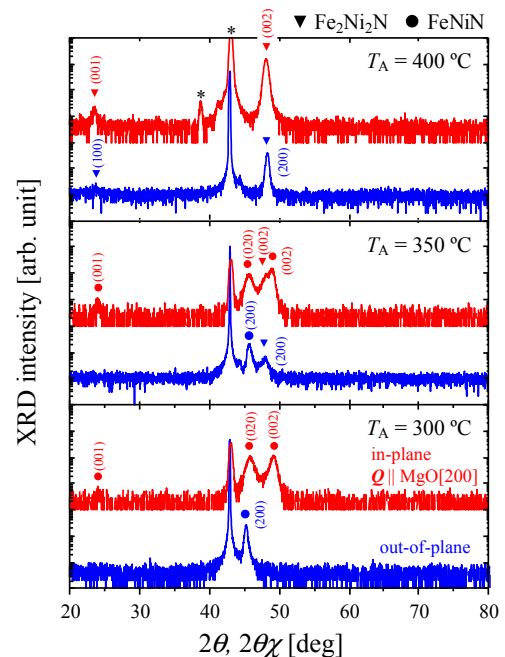


Fig. 3. (Color online) Out-of-plane (blue, lower) and in-plane XRD (red, upper) patterns of FeNiN film after annealed at $T_A = 300, 350,$ and 400 °C. Asterisks indicate diffraction peaks from the substrate.

of-plane ($2\theta-\omega$) and in-plane ($2\theta_\chi-\phi$) XRD patterns obtained after annealing at $T_A = 300, 350,$ and 400 °C. No notable change was found at $T_A = 300$ °C. When T_A was increased to 350 °C, we noted diffraction peaks from both Fe₂Ni₂N and FeNiN phases. When T_A was increased further to 400 °C, a single-phase Fe₂Ni₂N film was obtained. The S_N was determined to be 0.74, which was almost the same as Fe₂Ni₂N film shown in Fig. 2. This means that we succeeded in extracting approximately 50% of the N atoms from the FeNiN film by a simple post-annealing process. We note that the Fe₂Ni₂N film with extracted N atoms featured a tetragonal structure with $a = 3.788$ Å, $c = 3.768$ Å, and $c/a = 0.995$, which was different from the cubic one directly grown at $T_S = 450$ °C, as shown in Fig. 2. We presume that this tetragonal distortion indicates atomic ordering in the Fe₂Ni₂N film because the L1₀-FeNi alloy also has a small tetragonal distortion of $c/a \sim 1.007$.²⁰⁾

Figures 4(a) and 4(b) show the hysteresis curves of Fe₂Ni₂N films obtained by direct MBE growth at $T_S = 450$ °C and by extracting N atoms at $T_A = 400$ °C under vacuum from the FeNiN film grown at $T_S = 200$ °C, respectively. The magnetic fields were applied parallel ([100]) and perpendicular ([001]) to the substrate. In-plane easy magnetization with $M_S = 700 \pm 100$ emu/cm³ was confirmed in both films. Compared with Fig. 4(a), a larger magnetic field was required to saturate the magnetization perpendicular to the film plane in Fig. 4(b). This increase of the perpendicular saturation field of the Fe₂Ni₂N film also probably comes from atomic ordering. In our film, the L1₀ atomic ordering of the Fe and Ni atoms likely occurred parallel to the film plane, because the FeNiN film was grown with a -axis orientation. Hence, we assumed that the atomic ordering of Fe and Ni atoms in Fe₂Ni₂N enhanced the uniaxial magnetic anisotropy along the stacking direction of the Fe and Ni monolayers. If we can acquire c -axis oriented FeNiN film, uniaxial magnetic

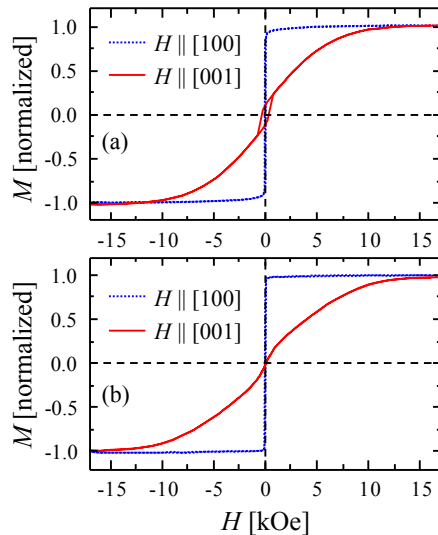


Fig. 4. (Color online) Hysteresis curves of $\text{Fe}_2\text{Ni}_2\text{N}$ films obtained by (a) direct growth at $T_S = 450^\circ\text{C}$ and (b) by N extraction from FeNiN film.

anisotropy of $\text{Fe}_2\text{Ni}_2\text{N}$ films increases in perpendicular to the film plane. $L1_0$ ordering of metallic atoms in anti-perovskite type ferromagnetic nitrides has a possibility to show PMA. We believe that this study could also make a major contribution to the formation of $L1_0$ -FeNi films by extracting 100% of the N atoms from FeNiN films.

In summary, we achieved epitaxial growth of single-phase FeNiN films on a MgO(001) substrate by MBE and then obtained atomically ordered $\text{Fe}_2\text{Ni}_2\text{N}$ films by extracting N atoms. The FeNiN films were grown with a -axis orientation, and therefore the atomic ordering of Fe and Ni atoms occurred parallel to the film plane. This work contributes to a new technique to form anti-perovskite type ferromagnetic

nitrides with an equiatomic ratio of metallic atoms, and the fabrication of high $L1_0$ -ordered FeNi films.

Acknowledgement Magnetization measurements were performed with the help of Professor H. Yanagihara of the University of Tsukuba.

- 1) R. N. Panda and N. S. Gajbhiye, *J. Appl. Phys.* **86**, 3295 (1999).
- 2) H. Y. Wang, J. H. S. Hang, W. H. Mao, H. Chen, H. Y. Zhang, Y. J. He, and E. Y. Jiang, *J. Appl. Phys.* **91**, 1453 (2002).
- 3) P. Prieto, J. Camarero, N. Sacristan, D. O. Boerma, and J. M. Sanz, *Phys. Status Solidi A* **203**, 1442 (2006).
- 4) G. Shirane, W. J. Takei, and S. L. Ruby, *Phys. Rev.* **126**, 49 (1962).
- 5) Y. Kong and F. Li, *Phys. Rev. B* **57**, 970 (1998).
- 6) S. K. Chen, S. Jin, T. H. Tiefel, Y. F. Hsieh, E. M. Gyorgy, and D. W. Johnson, Jr., *J. Appl. Phys.* **70**, 6247 (1991).
- 7) M. Kume, T. Tsujioka, K. Matsuura, Y. Abe, and A. Tasaki, *IEEE Trans. Magn.* **23**, 3633 (1987).
- 8) X. G. Diao, A. Y. Takeuchi, F. Garcia, R. B. Scorzelli, and H. R. Rechenberg, *J. Appl. Phys.* **85**, 4485 (1999).
- 9) F. Li, J. Yang, D. Xue, and R. Zhou, *Appl. Phys. Lett.* **66**, 2343 (1995).
- 10) P. Monachesi, T. Björkman, T. Gasche, and O. Eriksson, *Phys. Rev. B* **88**, 054420 (2013).
- 11) S. Kokado, N. Fujima, K. Harigaya, H. Shimizu, and A. Sakuma, *Phys. Rev. B* **73**, 172410 (2006).
- 12) A. Narahara, K. Ito, T. Suemasu, Y. K. Takahashi, A. Ranajikanth, and K. Hono, *Appl. Phys. Lett.* **94**, 202502 (2009).
- 13) Y. Komasaki, M. Tsunoda, S. Isogami, and M. Takahashi, *J. Appl. Phys.* **105**, 07C928 (2009).
- 14) Z. R. Li, W. B. Mi, and H. L. Bai, *Comput. Mater. Sci.* **142**, 145 (2018).
- 15) F. Takata, K. Ito, S. Higashikozono, T. Gushi, K. Toko, and T. Suemasu, *J. Appl. Phys.* **120**, 083907 (2016).
- 16) F. Takata, K. Kabara, K. Ito, M. Tsunoda, and T. Suemasu, *J. Appl. Phys.* **121**, 023903 (2017).
- 17) F. Takata, K. Ito, Y. Takeda, Y. Saitoh, K. Takanashi, A. Kimura, and T. Suemasu, *Phys. Rev. Mater.* **2**, 024407 (2018).
- 18) R. J. Arnott and A. Wold, *J. Phys. Chem. Solids* **15**, 152 (1960).
- 19) S. Goto, H. Kura, E. Watanabe, Y. Hayashi, H. Yanagihara, Y. Shimada, M. Mizuguchi, K. Takanashi, and E. Kita, *Sci. Rep.* **7**, 13216 (2017).
- 20) K. Takanashi, M. Mizugushi, T. Kojima, and T. Tashiro, *J. Phys. D* **50**, 483002 (2017).